

## EFFECT OF OXYGEN DURING THERMAL ANNEALING ON THE ELECTRICAL AND OPTICAL PROPERTIES OF SPUTTER DEPOSITED AL-DOPED ZNO FILMS FOR HETEROJUNCTION SOLAR CELL APPLICATION

Angelika Gorgulla, Nils Brinkmann, Daniel Skorka, Giso Hahn, Barbara Terheiden  
University of Konstanz, Department of Physics, 78457 Konstanz, Germany  
Phone: +49 7531 88 2080, Fax: +49 7531 88 3895, Email: angelika.gorgulla@uni-konstanz.de

**ABSTRACT:** The influence of oxygen during short post deposition annealing on Al-doped zinc oxide (AZO) films for heterojunction solar cells grown by sputter deposition is investigated in terms of their electrical, optical and structural properties. AZO films were annealed for 4 min at 300°C and 450°C in ambient air and N<sub>2</sub> atmosphere. It has been shown, that at 450°C the elimination of oxygen during annealing allows an increase in carrier concentration and reduction of the sheet resistance of AZO films four times higher than annealing in ambient air. This effect has not been observed for annealing temperatures below 300°C, where annealing in ambient air proved to have superior influence on the electrical properties. The optical bandgap of all annealed samples was enlarged and for an annealing temperature of 450°C the optical transmission weighted by ASTM G173-03 solar spectrum from 300 to 1100 nm was increased to over 80%. The changes observed in all samples were primarily explained by means of oxygen chemisorption and desorption processes. It is concluded, that oxygen plays an important role in the improvement of electrical and optical properties of AZO thin films during thermal annealing.

**Keywords:** TCO, AZO, thermal annealing, heterojunction solar cells

### 1 INTRODUCTION

The heterojunction solar cell concept, which employs stacked films composed of an intrinsic a-Si:H passivation and a doped a-Si:H emitter layer featuring front side contacts by transparent conductive oxides (TCOs), has attracted much attention due to its high conversion efficiency potential of 24.7% [1] and the fact, that the whole solar cell production process can be carried out at economical and energy efficient temperatures below 300°C [2]. Key advantage of heterojunction solar cells (HJS) is the high open circuit voltage, which can be attributed to the excellent passivation quality of the amorphous silicon used as emitter and BSF layer. Due to the low electric conductivity of a-Si:H, a TCO is needed at the front side of these solar cells in order to maintain a high lateral conductivity of the emitter layer. TCOs are commonly deposited by magnetron sputtering. To activate the a-Si:H passivation [3] and to cure damage induced on the a-Si:H layer during sputter deposition [4], a short annealing step below 300°C is required.

So far no thorough investigation has been carried out on the effect of oxygen during post deposition annealing on the electrical and optical properties of TCO films designed for heterojunction solar cells. As oxygen vacancies play a major role in the electrical transport in aluminum doped zinc oxide (AZO) [5], the elimination of oxygen in annealing environments might be a possibility to improve the transport properties of this TCO film and thus make it an alternative to the still widely used, but much more costly indium tin oxide (ITO) layer in highly efficient heterojunction solar cells. Despite the degrading effect of temperatures above 300°C on the passivation quality of amorphous silicon due to out-diffusion of hydrogen, annealing temperatures of 300°C and 450°C are investigated in order to illustrate the effect of oxygen during annealing on the electrical, optical and structural properties of AZO films.

### 2 EXPERIMENTAL

AZO films were deposited on borofloat glass at room temperature in a rf-13.56 MHz magnetron sputtering system (ATC-2200, AJA International). For film deposition a metallic Zn target doped with 2 wt% Al (99.99% pure) was used. The thickness of the deposited films was 150 nm as verified by profilometric measurements.

Prior to the sputtering process, all substrates were ultrasonically cleaned in acetone, isopropanol and deionized water sequentially. Afterwards, the substrates were dried with nitrogen gas. Before deposition, the sputtering chamber was evacuated to a base pressure of less than 10<sup>-6</sup> Torr. After a pre-sputtering period of 2 min under deposition conditions, the sputtering deposition was performed at a rf power of 5 W and a pressure of 2.5 mTorr for AZO deposition. Argon (20 sccm) was used as sputtering and oxygen (6 sccm) as reaction gas. During deposition, the substrates were rotated with constant speed for film uniformity. Annealing of the samples after deposition was performed in two different atmospheres at 300 and 450°C; on a hot plate in ambient air and in a tube furnace in nitrogen atmosphere under elimination of oxygen.

The electrical properties of the AZO films were characterized in terms of sheet resistance  $R_{\text{Sheet}}$  determined by four point probe measurements as well as free carrier density  $N_e$  and carrier mobility  $\mu_e$  derived from Hall measurements (HMS-5000, Ecopia) at room temperature using the van der Pauw method. The optical properties were characterized by spectral transmission and reflection measurements within a wavelength range of 300-2500 nm taken by a spectral photometer (Cary 5E, Varian) with air as reference. The optical band gap  $E_{\text{gap}}$  is calculated from the absorption coefficient, which has been derived from transmittance and reflectance spectra [5], by using Tauc's formula [6]. The crystalline structure of the films was analyzed by x-ray diffraction (XRD) (D8 XRPD, Bruker) using Cu K $_{\alpha}$  radiation (0.15418 nm).

### 3 RESULTS AND DISCUSSION

#### 3.1 Influence on electrical properties

For an annealing temperature of 300°C, AZO films annealed in both atmospheres show a decrease in sheet resistance  $R_{\text{Sheet}}$  during the first 4 min (Fig. 1). While at 450°C annealing in  $N_2$  atmosphere leads to an even stronger decrease of sheet resistance, the sample annealed in ambient air shows - following a drop after 2 min - a strong increase of sheet resistance after 4 min. The impact of oxygen on the properties of AZO films during annealing becomes clear considering the negative value of the relative change of the sheet resistance  $-\Delta_{\text{rel}}R_{\text{Sheet}}$  in dependence of temperature  $T_{\text{anneal}}$  after annealing for 4 min (Fig. 2). Annealing at 300°C in  $N_2$  atmosphere leads to a decrease in sheet resistance of 16%, annealing at 450°C reduces the sheet resistance by more than 32%. However, the opposite trend can be observed in ambient air, where annealing at 300°C improves the sheet resistance by 28%, annealing at 450°C by merely 8%.

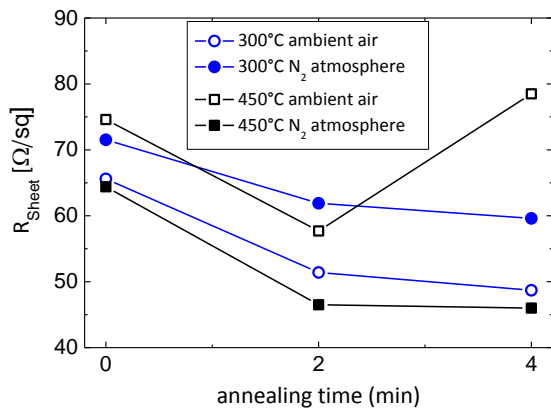


**Figure 1:** Sheet resistance of AZO films annealed at 300°C and 450°C in ambient air and  $N_2$  atmosphere.

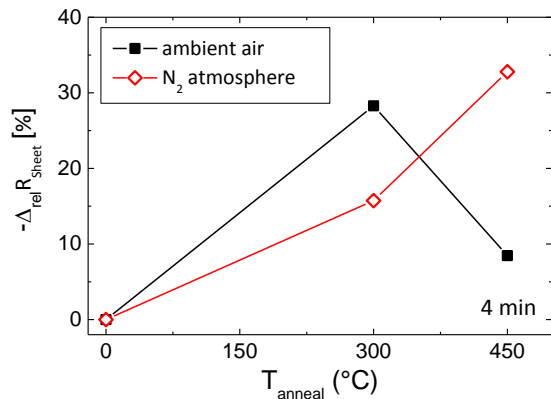


**Figure 2:** Relative change of sheet resistance of AZO films annealed for 4 min in ambient air and  $N_2$  atmosphere.

The reason for the observed behavior of the sheet resistance becomes apparent looking at the relative change of the free carrier density  $\Delta_{\text{rel}}N_e$  determined from Hall measurements (Fig. 3). While annealing at 300°C and 450°C has no significant effect on the free carrier mobility,  $\Delta_{\text{rel}}N_e$  resembles the trend of  $-\Delta_{\text{rel}}R_{\text{Sheet}}$ . The increase of carrier density at 300°C can be ascribed to electron release from oxygen vacancies and excess Zn interstitials [7]. It is well known, that in general the n-

type conduction of zinc oxide thin films is not only caused by substitutional donor atoms on zinc lattice sites (extrinsic donors), but also by native defects (intrinsic donors), such as interstitial zinc, hydrogen and in particular oxygen vacancies [8-11]. Oxygen vacancies within the AZO lattice can act as doubly charged electron donors and are therefore of major importance for the electric conductivity of this TCO [11].

As the annealing temperature is increased from 300 to 450°C in  $N_2$  atmosphere, the free carrier density increases from  $5 \cdot 10^{20}$  to  $7.2 \cdot 10^{20} \text{ cm}^{-3}$ . This change can be attributed to an enhanced electron release from oxygen vacancies [7] and/or generation of oxygen vacancies by oxygen desorption processes, which lead to a decrease of oxygen interstitials [12]. Interstitial oxygen acts as a trap center for free carriers and can become a dominating defect in ZnO [12-15].

In contrast, as the annealing temperature in ambient air is increased from 300 to 450°C, the carrier density decreases from  $6.2 \cdot 10^{20}$  to  $4.8 \cdot 10^{20} \text{ cm}^{-3}$ . It can be assumed, that annealing in ambient air leads to oxidation of the sample with two possible consequences. Firstly, chemisorption of oxygen at grain boundaries and the film surface and lead to an increase of interstitial oxygen, which results in an enhanced carrier recombination [7,12]. Secondly, by introducing oxygen into the film oxygen vacancies become saturated. It has been shown in previous studies, that annealing above 400°C in ambient air leads to a reduction of vacancies of ZnO and AZO films [7,14,16].

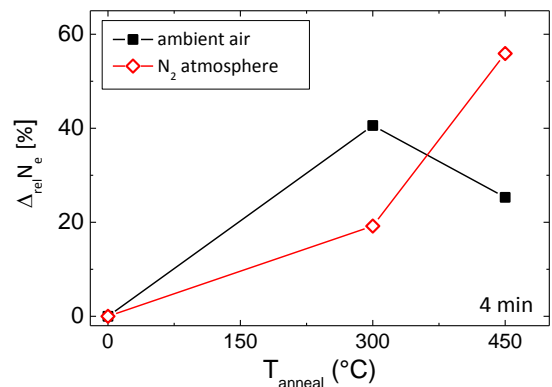


**Figure 3:** Relative change of free carrier density of AZO films annealed for 4 min in ambient air and  $N_2$  atmosphere.

#### 3.2 Influence on optical properties

Optical transmittance spectra and the transmittance weighted by ASTM G173-03 solar spectrum within a wavelength range (300-1100 nm) relevant for HJS for as-deposited and annealed AZO films are depicted in Fig. 4. Bare borofloat glass is shown as reference.

The absorption edge moves closer towards lower wavelength after annealing in both atmospheres at 300°C, but at 450°C the blue-shift of the absorption edge is more pronounced in  $N_2$  atmosphere than in ambient air. The blue-shift is a result of an enlargement of the optical band gap  $E_{\text{gap}}$  from around 3.40 eV for as-deposited samples to 3.49 eV (3.45 eV) in ambient air and 3.54 eV (3.62 eV) in  $N_2$  after annealing at 300°C (450°C) (Fig. 5). Considering the correlation between carrier density and optical band gap in our data, the increase of the band gap can be primarily attributed to the Burstein-Moss effect

[17,18], as in highly n-doped materials the lowest states of the conduction band are populated, resulting in a shift of the absorption edge towards shorter wavelengths. Compared to the film annealed at 450°C in N<sub>2</sub> atmosphere, the absorption edge of the film annealed in ambient air “red-shifts” to longer wavelengths, which is reflected in a narrowed band gap due to a lower carrier density.

The weighted optical transmission of AZO films increases with higher annealing temperature for both annealing atmospheres. As-deposited AZO films feature a weighted transmission around 76%, which increases to 78.2% (81.5%) after annealing in N<sub>2</sub> atmosphere and 78.6% (84%) by annealing in ambient air at 350°C (450°C). The increase of the weighted optical transmission is mainly due to an increase in transmission within the visible wavelength range (400-700 nm). The high optical transmission of the sample annealed in ambient air at 450°C can be attributed to the oxidation of the sample and to a decrease of oxygen vacancies, which are responsible for light absorption between 490 and 530 nm [19].

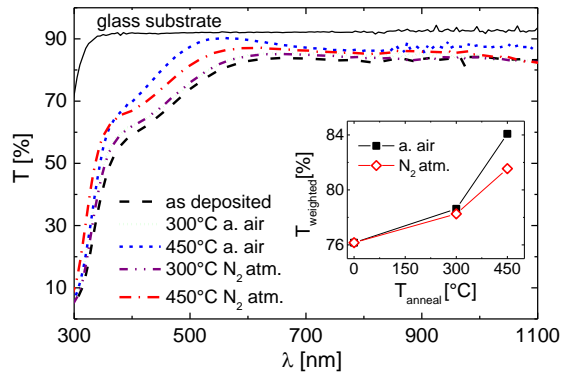


**Figure 4:** Optical transmission spectra and weighted transmission within a wavelength range relevant for HJS (300-1100 nm) of AZO films as-deposited and annealed for 4 min at 300°C and 450°C in ambient air and N<sub>2</sub> atmosphere.

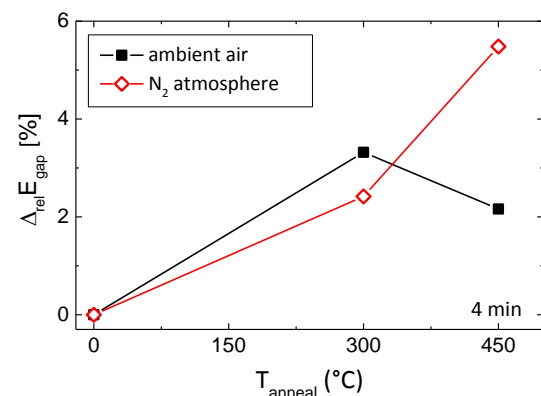


**Figure 5:** Relative change of optical band gap of AZO films for 4 min in ambient air and N<sub>2</sub> atmosphere.

Fig. 6 shows the optical transmission in the long wavelength range (1100-2500 nm). The decrease of IR transmission after annealing can be ascribed to free carrier absorption, which usually occurs at wavelengths above 1000 nm. The higher the carrier density the lower

the optical transmission of the AZO films (cf. Fig. 6 and N<sub>e</sub> values in section 3.1).

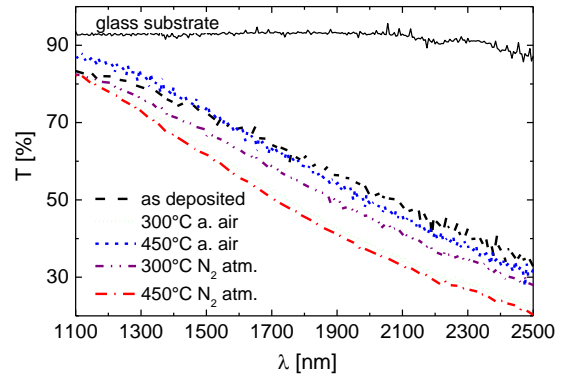


**Figure 6:** Optical transmission in long wavelength range of AZO films as-deposited and annealed for 4 min at 300°C and 450°C in ambient air and N<sub>2</sub> atmosphere.

### 3.3 Influence on structural properties

The annealing environment at a higher annealing temperature of 450°C proved to have a significant impact on the electrical and optical properties of AZO films. To investigate its influence on the structural properties, XRD measurements of as-deposited and AZO films annealed at 450°C have been performed within diffraction angles from 33° to 38° (Fig. 7). The XRD spectra exhibit broadened diffraction peaks indicating a nanocrystalline structure. Major diffraction peaks appear at around 34.5° and 35.8°, which can be assigned to reflections from (002) and (101) plains, respectively, of the hexagonal (wurtzite) phase of zinc oxide. The lattice constants were obtained as  $\bar{a} = 5.199 \text{ \AA}$  and  $\bar{c} = 3.306 \text{ \AA}$ .

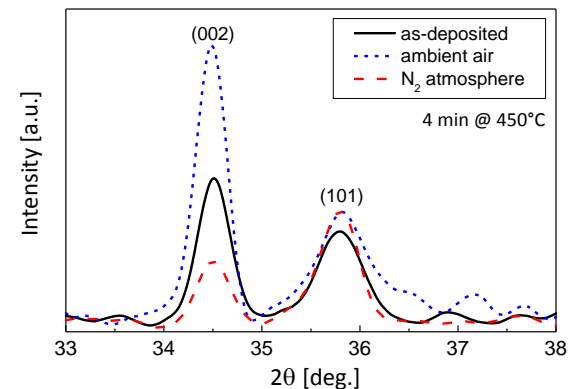


**Figure 7:** Noise reduced XRD patterns of AZO films as-deposited and annealed for 4 min at 450°C in ambient air and N<sub>2</sub> atmosphere.

Annealing in ambient air significantly increases the intensity of the (002) diffraction peak, while annealing in N<sub>2</sub> atmosphere decreases the peak intensity. The (101) diffraction peak intensity is only slightly increased regardless of annealing atmosphere. The mean crystallite sizes are derived from Scherrer’s equation with a measurement error of assumably less than 10%. The crystallite sizes of as-deposited and in ambient air annealed samples lie between 17 nm and 18 nm for the (101) orientation (Fig. 8). The sample annealed in N<sub>2</sub> atmosphere has a slightly increased (101) crystallite size of 22 nm. (002) oriented crystallites appear larger with

33 nm and 28 nm for as-deposited and in N<sub>2</sub> annealed samples, respectively.

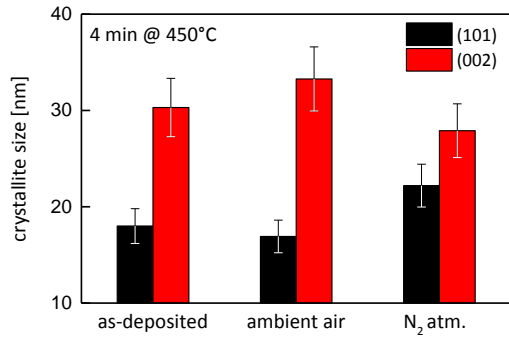


**Figure 8:** Crystallite sizes determined by Scherrer's equation of AZO films as-deposited and annealed for 4 min at 450°C in ambient air and N<sub>2</sub> atmosphere.

In accordance with the high peak intensity of the sample annealed in ambient air, a relatively large (002) crystallite size of 33 nm is noted, indicating a pronounced c-axis orientation. This can lead to the assumption of a better crystallized layer structure obtained by annealing in ambient air. However, the electron mobility, which is determined by both ionized impurity and grain boundary scattering, showed no significant change after temperature treatment in ambient air. This suggests an enhanced ionized impurity scattering after annealing in ambient air, which may be ascribed to interstitial oxygen acting as acceptors. To further investigate this issue non-uniform micro strain within the lattice has been considered, which is not taken into account by Scherrer's equation. The full-width at half-maximum (FWHM) can be expressed as a linear combination of the contribution from lattice strain and particle size. The effects of the strain and particle size on the FWHM can be deconvoluted by the following equation [20]

$$\frac{\beta \cos \theta}{\lambda} = \frac{1}{\varepsilon} + \frac{\eta \sin \theta}{\lambda}$$

where  $\beta$  is the FWHM measured in radians,  $\theta$  the Bragg angle of the peak,  $\lambda$  the x-ray wavelength,  $\varepsilon$  the effective particle size, and  $\eta$  the effective strain. Fig. 9 shows  $\beta \cos \theta / \lambda$  plotted against  $\sin \theta / \lambda$  (Williamson-Hall plot) for as-deposited and annealed samples for the two measured diffraction peaks.

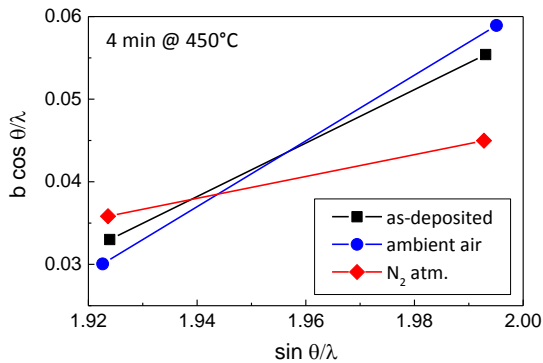


**Figure 9:** Williamson-Hall plot based on the data in Fig. 7 for AZO layers as-deposited and annealed for 4 min at 450°C in ambient air and N<sub>2</sub> atmosphere.

The effective strain can be estimated from the linear fit in Fig. 9. The positive slope of the fitted lines indicates a dominant tensile strain present within the AZO films [21]. This tensile strain becomes more pronounced by annealing in ambient air, but appears to become relieved by annealing in N<sub>2</sub> atmosphere. This coincides with the assumption that not only oxygen vacancies become saturated during annealing in ambient air at high temperature, but also interstitial oxygen is introduced into the lattice, which acts as a trap center and leads to an increase in tensile lattice strain. It is, however, important to note that it is not possible to make a reliable statement regarding the presence and effect of lattice strain within the present AZO films due to insufficient statistical data.

#### 4 SUMMARY

We have studied the influence of short thermal annealing in ambient air and N<sub>2</sub> atmosphere on the electrical, optical and structural properties of rf-magnetron sputtered AZO films designed for heterojunction solar cells. After annealing for 4 min at 300 and 450°C, the size of the optical bandgap and the spectral transmission within the VIS range were increased and the sheet resistance was decreased. At 300°C these changes were slightly more pronounced in ambient air than in N<sub>2</sub> atmosphere, but as the annealing temperature was increased to 450°C, annealing in N<sub>2</sub> atmosphere resulted in a reduction of the sheet resistance about four times higher than annealing in ambient air. Annealing in ambient air at 450°C, however, produced a slightly superior band gap widening and higher spectral transmission within the visible range. Hall measurements revealed that annealing primarily affects the charge carrier density, while it has little or no effect on charge carrier mobility. The widening of the optical band gap was for all samples attributed to the Burstein-Moss effect.

XRD measurements have shown, that AZO films annealed at 450°C in ambient air possess an enhanced (002) orientation and a better crystallized film structure compared to the sample annealed in N<sub>2</sub> atmosphere, which exhibits a less pronounced (002) orientation than the as-deposited sample. XRD measurements also indicated that films annealed in ambient air may contain more non-uniform tensile lattice strain, which can be attributed to an increase in oxygen interstitials. It is believed that the increase in sheet resistance and decrease of charge carriers in samples annealed in ambient air can be ascribed to chemisorption of oxygen at grain boundaries and film surface resulting in oxygen related trap centers and saturation of oxygen vacancies, which both lead to deterioration of the electrical film quality. The pronounced increase of carrier concentration at 450°C in N<sub>2</sub> atmosphere is attributed to the generation of oxygen vacancies due to thermal activation as well as oxygen desorption from the film.

From these results it is concluded that oxygen vacancies, which act as doubly charged electron donors, and oxygen interstitials acting as trap centers play an important role in the improvement of electrical and optical properties of AZO thin films. At a higher annealing temperature, the elimination of oxygen during annealing has proven to be beneficial for electrical conductivity. Further investigations are required regarding the issue whether the elimination of oxygen during annealing can be beneficial for AZO films in

heterojunction solar cells, as temperatures above 300°C have a degrading effect on the passivation quality of amorphous silicon layers.

## 5 ACKNOWLEDGEMENTS

Part of this work was financially supported by the German Federal Ministry for the Environment, Nature Conservation and Nuclear Safety (FKZ 0325581) and within the "REFINE" project from the Carl-Zeiss-Stiftung. The content is the responsibility of the authors.

## 6 REFERENCES

- [1] A. Yano et al., 28<sup>th</sup> EUPVSEC, Paris (2013) 748.
- [2] S. Taira et al., Proc. 22<sup>nd</sup> EUPVSEC (2007) 932.
- [3] S. De Wolf et al., Appl. Phys. Lett. 93 (2008) 32101.
- [4] D. Skorka et al., Proc. 28<sup>th</sup> EUPVSEC (2013) 1162.
- [5] D. Suwito, Dissertation, University of Konstanz, 2011.
- [6] J. Tauc, A. Menth, J. Non-Crystl. Solids 8 (1972) 569.
- [7] G. Fang et al., Phys. Stat. Sol. (a) 193 (2002) 139.
- [8] G. Tomlins et al., J. of Appl. Phys. 87 (200) 117.
- [9] D.C. Look et al., Phys. Rev. Lett. 82 (1999) 2552.
- [10] C.G. Van de Walle, Physica B: Condens. Matter 308-310 (2001) 899.
- [11] R. Vidya et al., Phys. Rev. B 83 (2001) 45206.
- [12] M. Bouderbala et al., Thin Sol. Films 517 (2009) 1572.
- [13] S. Takata et al., Thin Sol. Films 135 (1986) 183.
- [14] H. Fan et al., Chin. Phys. Lett. 24 (2007) 2108.
- [15] K.E. Knutsen et al., Phys. Rev. B 86 (2012) 121203.
- [16] J. Wang et al., ACS Applied Materials & Interfaces 4 (2012) 4024.
- [17] E. Burstein, Phys. Rev. 93 (1954) 632.
- [18] T.S. Moss, Proc. of the Phys. Soc. B 67 (1954) 775.
- [19] H.S. Kang et al., J. of Appl. Phys. 95 (2004) 1246.
- [20] W.H. Hall, Proc. Phys. Soc. A 62 (1949) 741.
- [21] C. Suryanarayana, M. Grant Norton, X-Ray diffraction: a practical approach, New York, Plenum Press, 1998.